# Simple few-shot method for spectrally resolving the wavefront of an ultrashort laser pulse

Slava Smartsev, Aaron Liberman, Igor A Andriyash, Antoine Cavagna, Alessandro Flacco, Camilla Giaccaglia, Jaismeen Kaur, Joséphine Monzac, Sheroy Tata, Aline Vernier, et al.

▶ **To cite this version:**

Slava Smartsev, Aaron Liberman, Igor A Andriyash, Antoine Cavagna, Alessandro Flacco, et al.. Simple few-shot method for spectrally resolving the wavefront of an ultrashort laser pulse. Optics Letters, 2024, 49 (8), pp.1900. 10.1364/OL.502000 . hal-04602907

**HAL Id: hal-04602907**
**https://hal.ip-paris.fr/hal-04602907**

Submitted on 6 Jun 2024

**HAL** is a multi-disciplinary open access archive for the deposit and dissemination of scientific research documents, whether they are published or not. The documents may come from teaching and research institutions in France or abroad, or from public or private research centers.

L'archive ouverte pluridisciplinaire **HAL**, est destinée au dépôt et à la diffusion de documents scientifiques de niveau recherche, publiés ou non, émanant des établissements d'enseignement et de recherche français ou étrangers, des laboratoires publics ou privés.

Distributed under a Creative Commons Attribution - NonCommercial 4.0 International License

Optics Letters

# Simple few-shot method for spectrally resolving the wavefront of an ultrashort laser pulse

Slava Smartsev,[1,†,*] Aaron Liberman,[2,†] Igor A. Andriyash,[1] Antoine Cavagna,[1] Alessandro Flacco,[1] Camilla Giaccaglia,[1] Jaismeen Kaur,[1] Joséphine Monzac,[1] Sheroy Tata,[2] Aline Vernier,[1] Victor Malka,[2] Rodrigo Lopez-Martens,[1] and Jérôme Faure[1]

[1]Laboratoire d'Optique Appliquée, ENSTA Paris, CNRS, Ecole Polytechnique, Institut Polytechnique de Paris, 828 Bd. des Maréchaux, Palaiseau 91120, France
[2]Department of Physics of Complex Systems, Weizmann Institute of Science, 234 Herzl St., Rehovot 7610001, Israel
[†]The authors contributed equally to this work.
*smartslava@gmail.com

Received 31 July 2023; revised 6 March 2024; accepted 12 March 2024; posted 12 March 2024; published 1 April 2024

**We present a novel, to the best of our knowledge, and straightforward approach for the spatio-spectral characterization of ultrashort pulses. This minimally intrusive method relies on placing a mask with specially arranged pinholes in the beam path before the focusing optic and retrieving the spectrally resolved laser wavefront from the speckle pattern produced at focus. We test the efficacy of this new method by accurately retrieving chromatic aberrations, such as pulse-front tilt (PFT), pulse-front curvature (PFC), and higher-order aberrations introduced by a spherical lens. The simplicity and scalability of this method, combined with its compatibility with single-shot operation, make it a strong complement to existing tools for high-intensity laser facilities.**

© 2024 Optica Publishing Group under the terms of the Optica Open Access Publishing Agreement

https://doi.org/10.1364/OL.502000

**Introduction**. Ultrashort lasers, with femtosecond pulse durations, are indispensable tools in medicine, industry, and science. The advent of chirped pulse amplification (CPA) [1] enabled such pulses to be amplified to peak powers of terawatts and even petawatts [2]. Intense, short laser pulses have opened possibilities to explore laser–matter interactions in the relativistic regime [3] and their applications as compact laser–plasma accelerators [4].

Ultrashort lasers are broadband and the spectral phase can impact the pulse's duration and shape in the temporal domain. Accurate and precise measurement of the spectral phase is the core of temporal metrology of ultrashort pulses [5]. Typical measurements assume that the spectral phase is not spatially varying.

High-intensity lasers, however, operate with large beams for which the spatio-spectral phase can be very important. Spatially non-uniform dispersion effects accumulated during amplification, propagation, and focusing can lead to different spectral components of the beam ending up with different wavefronts. These wavefronts determine how and where each color is focused, ultimately shaping the full multi-color spatiotemporal intensity at the focus. These and related effects are usually referred to as spatiotemporal couplings (STCs) [6].

The most commonly encountered STCs are pulse-front tilt (PFT), which can be caused by the misalignment of the gratings in the compressor, and pulse-front curvature (PFC), induced by chromatic lenses [7]. In most cases, STCs are undesirable because they increase pulse duration and reduce peak intensity and contrast at the focus [8]. In some cases, however, STCs can be exploited in a controlled and intricate way to manipulate the dynamics of intense pulses in the focal region [9,10]. Control over the velocity with which energy is deposited along the focal region, through the tailoring of STCs, paves the way toward a new generation of laser-driven particle accelerators [11–13] and X-ray sources [14]. Techniques for accurate and straightforward measurement of STCs are necessary to mitigate unwanted couplings and enable the utilization of STCs as a critical degree of freedom in an experiment.

The development of spatiotemporal metrology is well summarized in several reviews [6,15,16]. The main methods of STC characterization of ultrashort pulses are listed below.

(1) There are methods that utilize spectrally resolved wavefront measurements based on Shack–Hartmann sensors. HAMSTER, for instance, uses an acousto-optic programmable dispersive filter to isolate spectral components and then a Shack–Hartmann sensor to reconstruct each component's wavefront [17]. Other similar techniques employ optical filtering to narrow the pulse's spectral content [18,19].

(2) A number of methods are based on spatially resolved Fourier-transform spectroscopy (FTS). A self-referenced version of FTS, TERMITES [20,21], uses a spatially filtered copy of the beam as a clean reference for interference in the near field (NF). INSIGHT [22] uses a similar approach, but the interference is observed in the far field (FF), and the Gerchberg–Saxton (GS) iterative algorithm [23] is used to retrieve the spatially resolved spectral information of the beam.

(3) Some methods use hyperspectral imaging techniques for STC measurements. One example is broadband ptychography, which is based on coherent diffraction imaging. In ptychography, the beam under analysis is scattered off an object, forming a diffraction pattern. Phase retrieval algorithms are used to reconstruct the initial field from the diffraction patterns [24,25].

(4) Measurement methods such as RED-SEA-TADPOLE [26] characterize STCs by the spectral interference of the unknown test pulse with a known reference pulse.

(5) Yet another method, STRIPED-FISH [27], is based on holography and requires a spatially filtered reference beam. Recently, a similar method, CMISS [28], which does not require a special reference pulse, was proposed.

(6) Finally, there are STC measurement methods based on broadband Young's double-slit interferometry. The method relies on the fact that the far-field diffraction pattern of an ultrashort beam that impinges on Young's double slit (or two pinholes) contains information about the time delay between the two sub-pulses that go through the slits (or pinholes) [29,30].

While many of these techniques can effectively yield the spatiotemporal characterization of the beam, they generally have relatively complex experimental setups that can be expensive and challenging to install. Moreover, many of these methods rely on optical components that are not typically utilized in the beamline, such as beam splitters, bandpass filters, or gratings. As a result, they cannot be employed as *in situ* diagnostics, and their accuracy in representing the true spatiotemporal field of the experimental focal spot is limited. The most widely used techniques suffer from the need to take dozens or even hundreds of measurements, limiting their usefulness in high-power, low-repetition rate systems. The single-shot techniques, meanwhile, are often experimentally cumbersome. These limitations have made developing next-generation spatiotemporal measurement techniques a hot topic in the world of high-power lasers.

This Letter introduces an experimentally simple and novel method for measuring the multispectral wavefronts of ultrashort laser pulses in a single shot or only a few shots. IMPALA, or Iterative Multispectral Phase Analysis for LAsers, is based on the linear far-field interferometry of multiple beamlets generated by a special pinhole mask. Instead of a two-pinhole mask, we generalize Young's double-slit interferometry method to dozens of pinholes. The pinholes are arranged in a specific manner to ensure that each interference pattern created by any pair of holes does not overlap with others in the spatial Fourier plane, an idea inspired by phase retrieval in randomly positioned cores of a fiber bundle [31]. In one shot, it allows for the retrieval of spectrally resolved wavefronts of the ultrashort beam, spatially sampled at the pinhole positions. This is sufficient for low-spatial-resolution wavefront retrieval. In addition, rotations of the mask allow for improved spatial resolution of the wavefronts. This particular implementation of the pinhole mask was optimized to get a high spatial resolution from 12 shots, each with a unique rotation of the mask. Our method is remarkably straightforward because the only nonstandard optical element it requires is a special pinhole mask placed before the focusing optics used in the experiment. This mask can be easily cut or 3D printed. The method is minimally intrusive and can be readily moved in and out of an existing optical setup. It is easily scalable to different beam sizes, focal lengths of the optics, and spectral bandwidths. Thus, IMPALA combines scalability, a simple setup, low cost, and single-shot compatibility with sufficient spatial and spectral resolution for many applications.

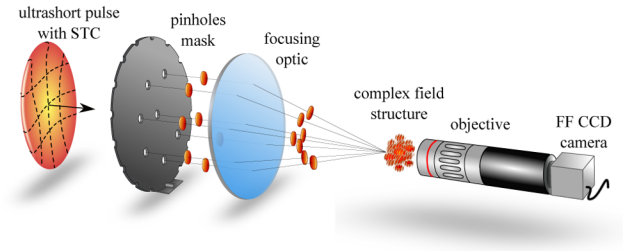


**Fig. 1.** Simplified experimental setup. A mask splits an ultrashort laser pulse with STCs into dozens of beamlets. A focusing optic concentrates the beamlets at its focal plane, which is then imaged by a microscope objective onto the FF CCD camera, thus registering the polychromatic FF intensity.

**Experimental methods and algorithm**. The simplified experimental setup is depicted in Fig. 1. An ultrashort laser pulse with unknown STCs impinges on the mask and is focused by a parabolic mirror or lens. A microscope objective images the optic's focal plane onto a CCD camera where the beamlets interfere and form a speckle pattern, shown in Fig. 2 as the polychromatic far-field (FF) intensity map. As we showed in [30], each pair of broadband beamlets forms a structured fringe pattern at the focus in the FF. The spatial fast Fourier transform (FFT) of this fringe pattern consists of a central peak and two sideband streaks, whose positioning depend on the beamlets' relative orientation. The length of the streaks depends on the bandwidth of the beam and also on the hole separation distance (see Eq. 16 in [30]). These streaks contain temporal information about the relative group delay between the beamlets. This is equivalent to a PFT estimate, which is proportional to the linear term in a spectrally resolved wavefront sampled at two spatial points. Generalizing this method allows for the extraction of the spectrally resolved wavefront, sampled at a dozen points. We obtain the optimal hole arrangement for a given number of holes and given laser spectrum using a genetic algorithm that packs the streaks with minimum overlap (see Supplement 1) to ensure proper phase retrieval.

The IMPALA algorithm is schematically shown in Fig. 2. The method is based on a measurement of the polychromatic FF intensity and utilizes the compact support constraint of the pinhole mask as a substitute for the NF amplitude [32]. The measured FF speckle intensity is Fourier transformed, and the resultant intensity (FFT{FF Intensity}) consists of sparse streaks. Different colors of the beam are distributed radially along these streaks. For example, along the same streak, the "redder" component (in our case $\lambda_R$ = 795 nm) is located closer to the center when compared to the "bluer" component ($\lambda_B$ = 758 nm), and the central component ($\lambda_0$ = 772 nm) is between them. This is due to the fact that the "redder" monochromatic speckle pattern has a smaller spatial frequency, which is inversely proportional to the wavelength. This separation allows us to isolate monochromatic "spots" inside the polychromatic streaks (see Supplement 1). These isolated spots (and their corresponding phases and amplitudes) inside of the Fourier-transformed speckle intensity are spatially transformed back to obtain a monochromatic speckle pattern. Having obtained a monochromatic intensity in the FF and using the constrained compact support of the pinhole mask to substitute the mask transmission function (value of 1 at the holes, 0 everywhere else) for the NF amplitude, we use the GS algorithm to find the spatial phase

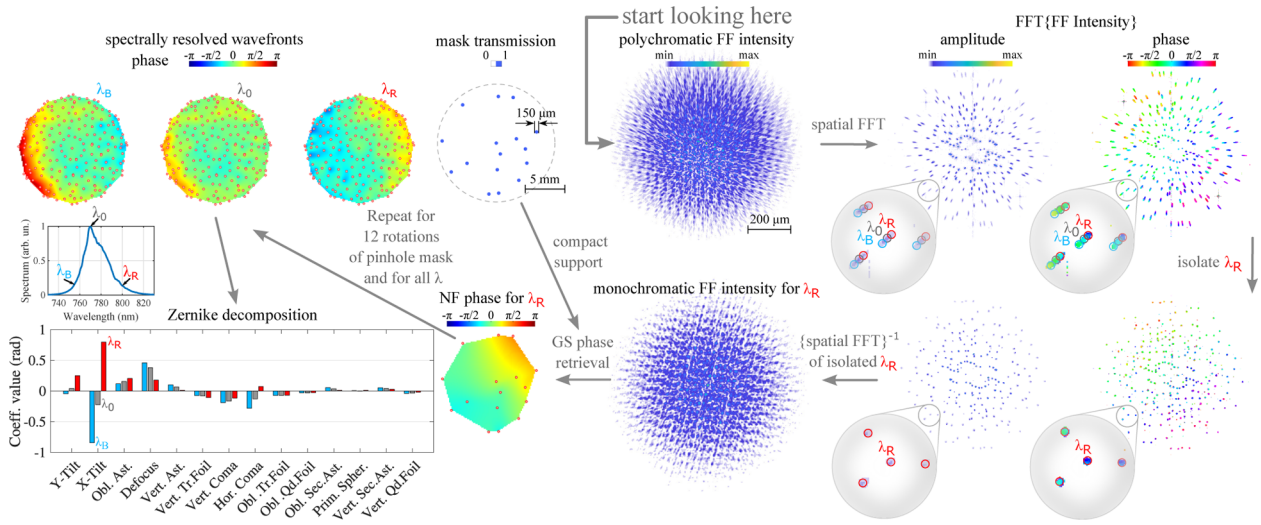


**Fig. 2.** Algorithm structure and sample wavefront retrieval. The monochromatic FF intensity is extracted from the measured polychromatic FF intensity by utilizing the spatial separation of the colors in the streaks. The GS algorithm reconstructs the NF phase of the beamlets using the mask transmission function (value of 1 at holes, 0 everywhere else) as compact support for the NF amplitude. The process is repeated for different colors and mask rotations to obtain spectrally resolved wavefronts, from which the Zernike coefficients of the analyzed wavefronts are extracted.

(and amplitude: see Supplement 1) in the NF for each specific color. The process is then repeated for different colors to obtain a spectrally resolved wavefront. The spatial resolution is enhanced by rotating the mask over 12 angular positions, obtaining more dense spatial sampling in the NF. It should be noted that the hole placement in the mask was optimized to balance between the sparsity of the speckle intensity in the Fourier plane (avoid overlapping streaks) and uniform sampling of holes in the NF when summing all 12 rotations (see Supplement 1).

The length of the polychromatic streak (along the radial coordinate) defines the spectral resolution of the phase measurement. Drawing from the model derived in [30], we show in Supplement 1 that the spectral resolution is $\Delta\lambda_{impala} \approx \Delta\lambda(1 + [\Delta\lambda s_b/\sqrt{2\log 2}\lambda_0 d_b]^2)^{-1/2}$, where $\Delta\lambda$ and $\lambda_0$ are the full width at half maximum (FWHM) of the spectrum and its central wavelength, while $s_b$ and $d_b$ are the beamlets' separation and diameter (or hole diameter) in the NF, respectively. For the longest streaks in Fig. 2, the spectral resolution is $\Delta\lambda_{impala} \approx 10$ nm, using the experimentally relevant parameters $\Delta\lambda = 30$ nm, $\lambda_0 = 770$ nm, $s_b = 12$ mm, and $d_b = 150$ μm.

It should be noted that IMPALA, as a linear measurement, requires a nonlinear measurement of the spectral phase in order to stitch together the monochromatic wavefronts.

**Results and discussion**. The experiments were performed at Laboratoire d'Optique Appliquée using the Salle Noire 3.0 laser system. The laser's front end consists of a commercial Ti:Sa oscillator (Rainbow, Femtolasers GmbH), followed by a Ti:Sa chirped pulse amplifier system (Femtopower Pro-HE) delivering 30 fs compressed pulses of up to 1.2 mJ energy with a 1 kHz repetition rate. We used a standard cube polarizer–wave plate pair attenuator to obtain a variable attenuation of the beam in the range of hundreds of μJ without introducing any STC between the measurements. In addition, a neutral density filter with an optical density of 4 was installed before the FF CCD sensor during all measurements. To avoid any risk of nonlinear effects, we stretched the pulse to nearly 1 ps by introducing GDD through an acousto-optic programmable dispersive filter

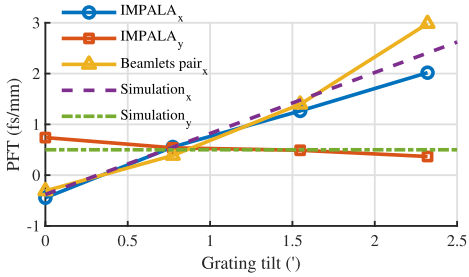


**Fig. 3.** Measured and simulated introduced PFT as a function of a grating tilt of the compressor.

(Dazzler, Fastlite) integrated into the main amplifier. We tested IMPALA by measuring the spectrally resolved wavefronts of the laser. For further testing, we introduced STCs into the laser in a controlled way and retrieved them with IMPALA, thus verifying the correctness of our method.

*Parabolic mirror as a focusing optic and introduced PFT*. We tested our method by introducing a controlled amount of PFT by acting on the parallelism of the compressor gratings in their dispersion plane (see Supplement 1). The focusing element, in this case, was a 100 mm focal length, 90° off-axis parabolic mirror. As seen in Fig. 3, we observe a linear PFT as a function of grating misalignment in the $x$ axis (grating dispersion plane), while the PFT in the $y$ axis is nearly constant. The slight variation can be explained by an imperfect alignment of the compressor's roof mirrors, which can couple the $x$ and $y$ axes for the PFT. In addition, we estimate the PFT with our previous method based on the interference of two beamlets by using a mask with two holes [30]. The IMPALA's PFT measurement agrees both with the measured PFT using the beamlet method and the simulation. The measured wavefronts for a grating tilt of 2.3' (minutes of arc) and their Zernike decomposition are shown in Fig. 2.

*Singlet lens as a focusing optic and introduced PFC*. We also tested IMPALA by using a spherical singlet lens as a focusing element. A singlet lens introduces PFC when focusing an

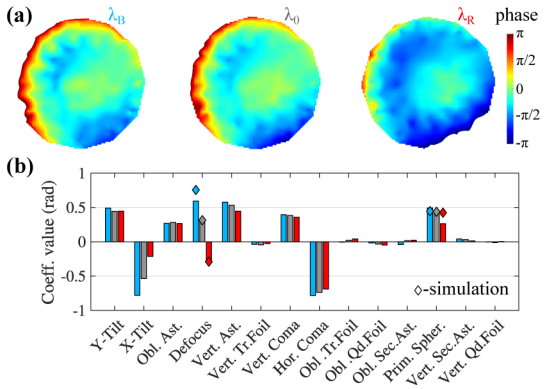


**Fig. 4.** Measured wavefronts (a) and their Zernike decomposition (b) for experiments with a singlet lens as a focusing optic. Predicted chromatic defocus and spherical terms of the lens are shown as diamonds.

ultrashort pulse since it has a non-negligible amount of longitudinal chromatic aberration [7]. We used a 100 mm focal length plano–convex singlet lens as the focusing element (see Supplement 1). The measured spectrally resolved wavefronts are depicted in Fig. 4(a). These spatial phase fronts were unwrapped manually at a few points by adding or removing $2\pi$. The displayed phase range is limited to $2\pi$ to make the spherical term visible. From the Zernike decomposition shown in Fig. 4(b), it is evident that the lens introduces non-negligible chromatic defocus terms, observable in the measurement through the chromatically dependent defocus term. This corresponds to a PFC of $\mathrm{PFC}_{meas\ singlet} = 0.20\,\mathrm{fs/mm^2}$ (while the predicted $\mathrm{PFC}_{pred\ singlet} = 0.23\,\mathrm{fs/mm^2}$). For comparison, the value of the PFC in the measurement with the parabola, shown in Fig. 2, is $\mathrm{PFC}_{parab} = 0.052\,\mathrm{fs/mm^2}$. Additionally, the lens introduces the expected spherical aberration, and the measured value quantitatively aligns well with the simulation (diamonds in Fig. 4). The other measured aberration terms (astigmatism and coma) are probably mainly due to imperfect lens alignment. The nonzero value of the $\mathrm{PFC}_{parab}$ is expected and reflects the fact that there is a chromatic beam expander in the laser chain.

**Conclusion**. We presented a simple yet powerful method to measure spectrally resolved wavefronts of broad-spectrum lasers. We successfully tested our method by inducing controlled STCs and demonstrating their accurate measurement. Our method performed well both when compared to simulations and when benchmarked against a previous measurement method. This method is extremely simple to implement and to scale to different systems and is compatible with high-power, low-repetition rate laser systems. We hope IMPALA will be useful in high-power laser laboratories, potentially helping in making STC measurements as common a part of laser diagnostics as spatial wavefront and temporal measurements are today.

**Funding.** WIS-CNRS (IPR LAMA); Dita and Yehuda Bronicki; R. Lapon; Schilling Foundation; Wolfson Foundation; Minerva; Israel Science Foundation; Benoziyo Endowment Fund for the Advancement of Science; Schwartz/Reisman Center for Intense Laser Physics; Laserlab-Europe (871124); Agence Nationale de la Recherche (ANR-10-LABX-0039-PALM, ANR-20-CE92-0043-01); Advanced Grant ExCoMet (694596); Horizon 2020 Framework Programme (101004730).

**Acknowledgment.** We thank Prof. Dan Oron for the fruitful discussions. We also thank Dr. Nicolas Thurieau for printing the masks and Sébastien Brun and Pascal Rousseau for assistance in micro-drilling.

**Disclosures.** The authors declare no conflicts of interest.

**Data availability.** The data supporting this study's findings are available from the authors upon reasonable request.

**Supplemental document.** See Supplement 1 for supporting content.

## REFERENCES

1. D. Strickland and G. Mourou, Opt. Commun. **56**, 219 (1985).
2. C. N. Danson, C. Haefner, J. Bromage, *et al.*, High Power Laser Sci. Eng. **7**, e54 (2019).
3. G. Mourou, T. Tajima, and S. V. Bulanov, Rev. Mod. Phys. **78**, 309 (2006).
4. E. Esarey, C. B. Schroeder, and W. P. Leemans, Rev. Mod. Phys. **81**, 1229 (2009).
5. I. A. Walmsley and C. Dorrer, Adv. Opt. Photonics **1**, 308 (2009).
6. S. Akturk, X. Gu, P. Bowlan, *et al.*, J. Opt. **12**, 093001 (2010).
7. Z. Bor, Opt. Lett. **14**, 119 (1989).
8. C. Bourassin-Bouchet, M. Stephens, S. de Rossi, *et al.*, Opt. Express **19**, 17357 (2011).
9. A. Sainte-Marie, O. Gobert, and F. Quéré, Optica **4**, 1298 (2017).
10. D. H. Froula, D. Turnbull, A. S. Davies, *et al.*, Nat. Photonics **12**, 262 (2018).
11. A. Debus, R. Pausch, A. Huebl, *et al.*, Phys. Rev. X **9**, 031044 (2019).
12. C. Caizergues, S. Smartsev, V. Malka, *et al.*, Nat. Photonics **14**, 475 (2020).
13. J. P. Palastro, J. L. Shaw, P. Franke, *et al.*, Phys. Rev. Lett. **124**, 134802 (2020).
14. A. Kabacinski, E. Oliva, F. Tissandier, *et al.*, Nat. Photonics **17**, 354 (2023).
15. C. Dorrer, IEEE J. Sel. Top. Quantum Electron. **25**, 3100216 (2019).
16. S. W. Jolly, O. Gobert, and F. Quéré, J. Opt. **22**, 103501 (2020).
17. S. L. Cousin, J. M. Bueno, N. Forget, *et al.*, Opt. Lett. **37**, 3291 (2012).
18. Y. G. Kim, J. I. Kim, J. W. Yoon, *et al.*, Opt. Express **29**, 19506 (2021).
19. N. Weiße, J. Esslinger, S. Howard, *et al.*, "Measuring spatio-temporal couplings using modal spatio-spectral wavefront retrieval," arXiv, arXiv.2303.01360 (2023).
20. M. Miranda, M. Kotur, P. Rudawski, *et al.*, Opt. Lett. **39**, 5142 (2014).
21. G. Pariente, V. Gallet, A. Borot, *et al.*, Nat. Photonics **10**, 547 (2016).
22. A. Borot and F. Quere, Opt. Express **26**, 26444 (2018).
23. R. W. Gerchberg, Optik **35**, 237 (1972).
24. D. J. Batey, D. Claus, and J. M. Rodenburg, Ultramicroscopy **138**, 13 (2014).
25. D. Goldberger, J. Barolak, D. Schmidt, *et al.*, Opt. Lett. **48**, 3455 (2023).
26. V. Gallet, S. Kahaly, O. Gobert, *et al.*, Opt. Lett. **39**, 4687 (2014).
27. P. Gabolde and R. Trebino, Opt. Express **14**, 11460 (2006).
28. Y. Xu, Y. Yi, P. Zhu, *et al.*, Opt. Lett. **47**, 5664 (2022).
29. R. Netz and T. Feurer, Appl. Phys. B **70**, 813 (2000).
30. S. Smartsev, S. Tata, A. Liberman, *et al.*, J. Opt. **24**, 115503 (2022).
31. D. Kogan, S. Sivankutty, V. Tsvirkun, *et al.*, Opt. Lett. **42**, 647 (2017).
32. J. R. Fienup, *Phase Retrieval and Image Reconstruction for Astronomy. Image Recovery: Theory and Application* (Academic Press, 1987).

78.196.74.251 {ts '2024-06-06 03:06:23'}